

Study of Grain-Growth Kinetics in Delta-Ferrite and Austenite with Application to Thin-Slab Cast Direct-Rolling Microalloyed Steels

TIHE ZHOU, RONALD J. O'MALLEY, and HATEM S. ZUROB

The high-temperature grain-growth kinetics in delta-ferrite and austenite is investigated. The delta-ferrite growth kinetics was observed directly on a model alloy that contained 2.5 wt pct aluminum in order to stabilize delta-ferrite down to room temperature. The gamma grain-growth kinetics was by etching the former austenite grain boundaries in a precipitate-free variant of APIX60 steel. At high temperatures and in the absence of precipitation, the growth kinetics in both delta-ferrite and austenite appeared to follow a simple parabolic growth law. The findings are applied to the problem of grain-size control during the process of thin-slab casting direct rolling (TSCDR).

DOI: 10.1007/s11661-010-0246-y

© The Minerals, Metals & Materials Society and ASM International 2010

I. INTRODUCTION

THE direct linking of casting and hot rolling through thin-slab casting direct-rolling (TSCDR) technology has the advantages of reducing capital, energy, labor, and inventory costs, as well as the ability to roll thinner strip compared to the route of thick slab casting, reheating, and hot rolling.^[1] Recently, much emphasis has been placed on using this process to produce high grade microalloyed steels that can comply with the American Petroleum Institute (API) standards.^[2] At present, TSCDR technology can only be used to produce APIX60 and APIX70. Production of higher grades, such as APIX80, proved to be very difficult due to the presence of extremely large γ grains in the center of the slab prior to thermomechanical processing.^[3,4] The limited number of thermomechanical deformation passes available in the case of thin slabs can make it difficult to refine these larger grains.^[5–10] In order to get uniform and finer microstructure, control of as-cast as well as solid-state microstructure evolution is extremely important.^[6] In this contribution, we focus on grain growth in the delta-ferrite and austenite prior to the start of thermomechanical processing. Very little information on grain growth is available at these high temperatures, because the delta-ferrite and austenite grains are not retained on quenching to room temperature. In this work, a model alloy in which the delta-ferrite is stable down to room temperature is used to study grain growth in the delta phase. Grain growth in austenite is studied by etching the former austenite grain boundaries of an Nb- and Ti-free version of APIX60 steel.

II. EXPERIMENTAL PROCESS

Direct observation of the grain growth in delta-ferrite is extremely difficult because delta-ferrite transforms to austenite and subsequently martensite on quenching. Standard metallographic techniques are unable to reveal the former delta grain boundaries, thus rendering investigation of grain growth extremely difficult. In order to study the kinetics of grain growth in delta-ferrite, a model alloy with 2.5 wt pct Al was used. The addition of Al is based on the fact that Al is the most efficient ferrite stabilizer. An addition of as little as 2.5 wt pct Al is sufficient to avoid austenite formation and retain ferrite down to room temperature, as shown in Figure 1. The composition of the alloy used to study grain growth in delta-ferrite growth is shown in Table I. This alloy will be referred to as the “Fe-Al model” alloy to remind the reader that this alloy is not intended for industrial use; it is simply used to allow direct measurement of ferrite grain-growth kinetics in a system, which is comparable to industrial alloys.

The model alloy was prepared by arc melting small ingots of 20 to 30 g in an argon atmosphere. The as-cast delta grain size was as large as 2000 μm and, as such, unsuitable for studying the kinetics of grain growth. In order to refine the grain size, the as-cast specimen was annealed at 923 K (650 °C) for 2 hours and then cold deformed and recrystallized 3 times* to obtain a

*The recrystallization treatment consisted of cold rolling followed by annealing at 1023 K (750 °C). The cold reduction steps were 30, 55, and 55 pct. The annealing times were 4 h after the first and second reductions and 8 h after the third reduction.

uniform grain size of 27 μm , as shown in Figure 2. In one batch of samples, the grain size achieved was higher, 183 μm . This higher initial grain size was taken into account during subsequent modeling.

TIHE ZHOU, Postdoctoral Student, and HATEM S. ZUROB, Assistant Professor, are with the Steel Research Centre, McMaster University, Hamilton, ON, Canada, L8S 4L7. Contact e-mail: zurabh@mcmaster.ca RONALD J. O'MALLEY, Plant Metallurgist, is with Nucor Steel Decatur, LLC, Decatur, AL 35609.

Manuscript submitted September 17, 2009.

Article published online May 22, 2010

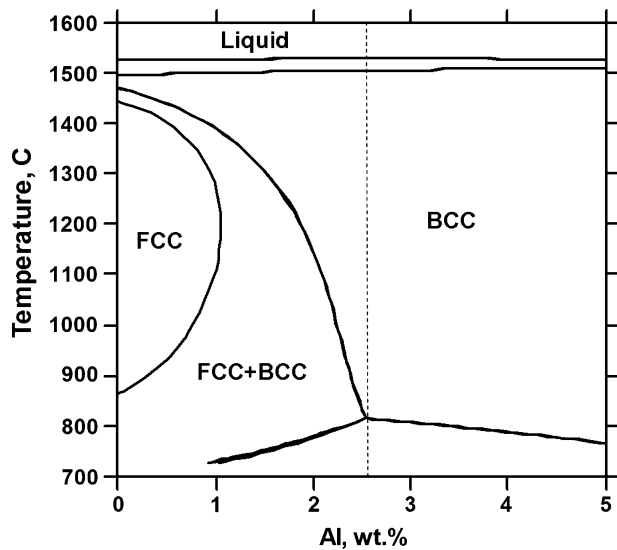


Fig. 1—Effect of Al addition on phase stability of a steel containing Fe-0.0531 pct C-1.0954 pct Mn-0.205 pct Si. A model alloy with 2.5 pct Al is chosen for the study of grain growth in delta-ferrite.

Table I. Chemical Composition of Experimental Materials

| Wt pct | C | Mn | Si | Al | Ti | Nb | N |
|------------------------|--------|--------|-------|-------|--------|-------|--------|
| Thin slab APIX60 | 0.0531 | 1.0954 | 0.205 | 0.021 | 0.0085 | 0.032 | 0.0093 |
| Fe-Al model alloy | 0.053 | 1.10 | 0.4 | 2.5 | 0 | 0 | 0 |
| Nb/Ti-free model alloy | 0.0527 | 1.12 | 0.205 | 0 | 0 | 0 | 0 |

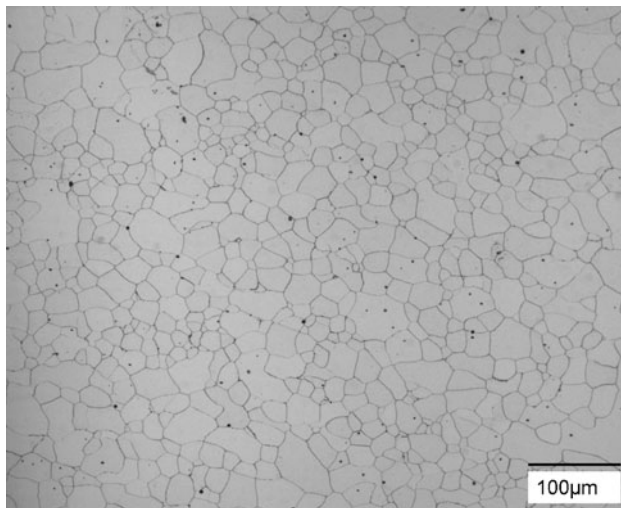


Fig. 2—As-cast Fe-Al model alloy was cold deformed and recrystallized 3 times to obtain a uniform grain size of about 27 µm.

The grain-refined model alloy was heated to temperatures of 1273 K (1000 °C), 1373 K (1100 °C), 1473 K (1200 °C), 1573 K (1300 °C), and 1743 K (1470 °C) and

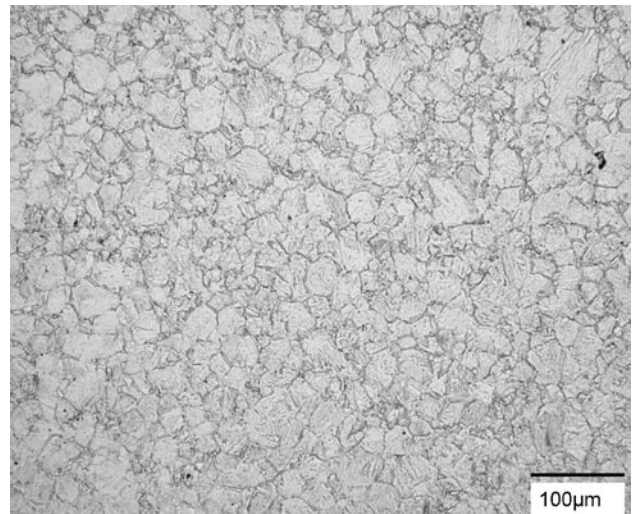


Fig. 3—Nb/Ti-free alloy used for investigating grain growth in austenite. The austenite grain size at the beginning of the grain-growth experiments (*i.e.*, at 1173 K (900 °C)) was 40 µm.

held at temperature for different times before being quenched in ice water. The complete thermal history of each sample was recorded using a B-type thermocouple and an acquisition frequency of 7.5 Hz. The annealing treatments were carried out under an atmosphere of CO-CO₂ whose carbon activity corresponds to that of the alloy at the isothermal holding temperature. This was essential in order to avoid decarburization of the specimen during the annealing treatments. The ferrite grain structure in the model alloy was revealed using an etching solution of supersaturated picric acid with sodium dodecylbenzene sulfonate wetting agent.

Observation of austenite grain growth was carried out on a second alloy, which is an Nb- and Ti-free version of APIX60 steel. This alloy is used in place of the standard APIX60 chemistry, because abnormal grain growth took place in the standard alloy due to the dissolution of the precipitates on reheating. The use of a “precipitate-free” alloy avoids this complication. The alloy used for the austenite grain-growth experiments was prepared by arc melting, and its composition is shown in Table I. The as-cast material was homogenized for 3 days at 1373 K (1100 °C) to break down the as-cast microstructure. Two cycles of austenitization at 1148 K (875 °C) for 15 minutes followed by quenching in ice water were used to refine the grain size. In order to estimate the initial austenite grain size for subsequent grain-growth experiments, one of the grain-refined specimens was heated to 1173 K (900 °C) and quenched; the austenite grain size of this specimen was found to be 40 µm, as shown in Figure 3. This was used as the initial grain size in the subsequent austenite grain-growth experiments, which were carried out using this refined Nb/Ti-free alloy in the austenite range at temperatures of 1473 K (1200 °C), 1573 K (1300 °C), and 1673 K (1400 °C). As before, the complete thermal history was recorded for each specimen and an appropriate CO-CO₂ atmosphere was used to prevent decarburization. The former austenite grain boundaries were revealed using an aqueous

solution of picric acid with sodium dodecylbenzene sulfonate and different additions of hydrochloric acid for the different annealing temperatures.^[5,11]

In all cases, the grain size was measured using the linear intercept method and the true three-dimensional grain diameter was calculated as 1.61 times the linear intercept diameter.^[12]

III. RESULTS

The use of the Fe-Al model alloy permitted accurate determination of the grain size evolution, as shown in Figure 4, which shows the grain size evolution of specimens held at 1373 K (1100 °C) for times of 360, 480, and 1180 seconds. The times given represent the total time, including heating time, which can be a significant fraction of the total time, as shown by the thermal profile in Figure 4(d). As such, the measured grain-growth kinetics is not strictly isothermal and the complete thermal profile needs to be analyzed in order to quantitatively interpret the grain-growth data. A

detailed analysis, which takes into account the effect of the heating rate, is presented in the discussion section. For convenience, the grain-growth data are summarized in Figure 5 using the total time in the furnace.

Similar results were obtained for austenite grain growth in the Nb/Ti-free model alloy. Figure 6 summarizes the austenite grain-growth kinetics measured by etching the former austenite grain boundaries. Once again, the time refers to the total time in the furnace, including the heating time. An example of the austenite grain size evolution at 1573 K (1300 °C) for times of 5 and 15 minutes is shown in Figure 7.

IV. DISCUSSION

A. Grain Growth in Delta-Ferrite

In order to facilitate the study of grain growth in delta-ferrite, a model alloy with 2.5 wt pct Al was prepared in order to stabilize delta-ferrite down to room temperature. Thermodynamic calculations using the TCFE2 database

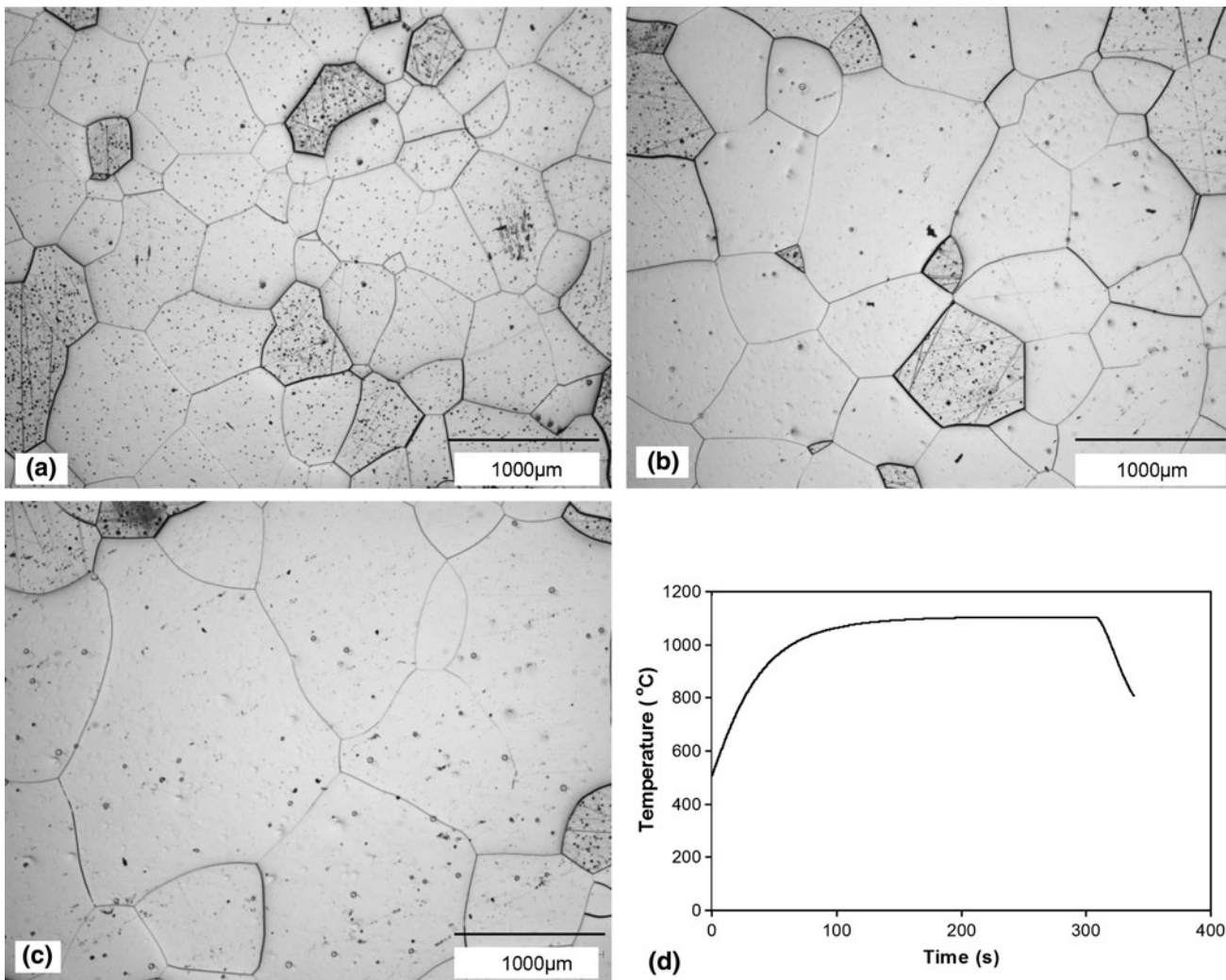


Fig. 4—Microstructure of Fe-Al model alloy after heating to 1373 K (1100 °C) for (a) 360 s, (b) 480 s, and (c) 1180 s. The heating profile was recorded for each sample, as illustrated in (d).

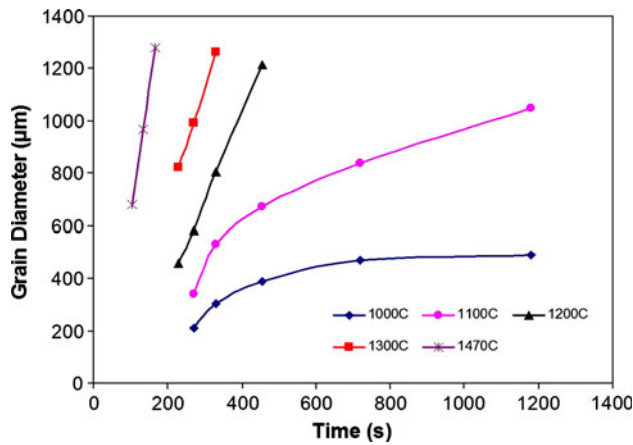


Fig. 5—Summary of the measured delta-ferrite grain-growth kinetics measured in the Fe-Al model alloy. The solid lines are added to guide the eye.

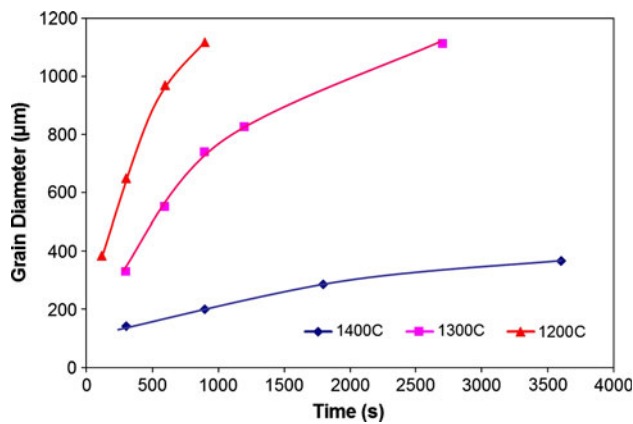


Fig. 6—Summary of the austenite grain-growth kinetics measured by etching the former austenite grain boundaries in the Nb/Ti-free alloy. The solid lines are added to guide the eye.

of THERMO-CALC**^[13] indicate that the Al is in solid

**THERMO-CALC is a trademark of Thermo-Calc, Stockholm.

solution and, as such, would not contribute any additional precipitate pinning compared to the Al-free alloy.^[14] At the same time, it is unlikely that Al would exert strong solute drag at the migrating grain boundaries at the very high temperatures being investigated in this work.^[15] For these reasons, it is argued that the addition of Al should not modify the grain-growth kinetics of the model alloy compared to Al-free steel. It should also be pointed out that, unlike conventional APIX60 steels, the model alloy does not contain Nb or Ti additions. Once again it is argued that this difference is not significant, because the solute-drag effect of these elements was shown to be negligible^[16] at temperatures above 1473 K (1200 °C). Furthermore, the volume fraction of microalloyed precipitates in the delta region in conventional steels is very small and, as such, the Zener pinning effect is small.

In order to model the grain-growth kinetics including the effect of heating time, a simple nonisothermal grain-growth model is used. The growth rate is assumed to be proportional to the driving force due to the curvature of the grains:^[17]

$$\frac{dr}{dt} = M(t) \frac{2\gamma}{r} \quad [1]$$

In this equation, r is the radius of the grain, $M(t)$ is the grain boundary mobility, and γ is the grain boundary energy. The grain boundary mobility is a function of time, t , in order to capture the change in temperature during heating. Integration of Eq. [1] leads to

$$r^2 = r_0^2 + 4\gamma \int_0^t M(t) dt \quad [2]$$

where r_0 is the initial grain radius, which is 13.5 μm , as shown in Figure 2. As mentioned in Section II, one

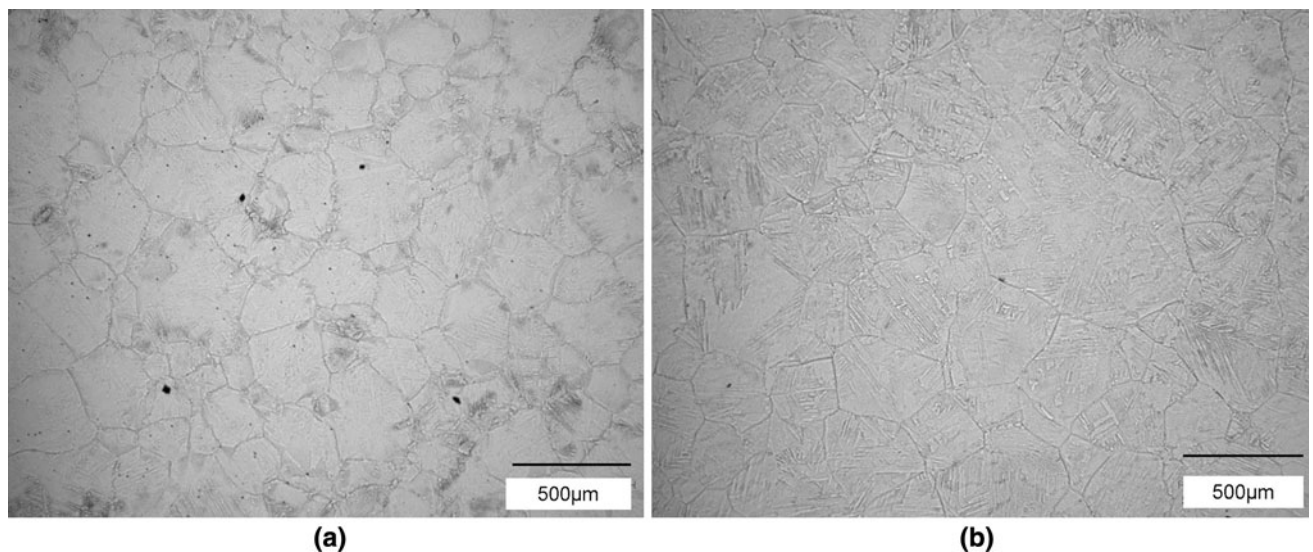


Fig. 7—Evolution of the austenite grain size at 1573 K (1300 °C) for holding times of (a) 5 min and (b) 15 min.

batch of samples had an initial grain size of $r_0 = 91.5 \mu\text{m}$. This batch was used for grain-growth experiments at 1273 K (1000 °C) and 1373 K (1100 °C), and as such, r_0 is $91.5 \mu\text{m}$ in these two cases.

The Turnbull mobility^[18] was used as an initial estimate of the grain-boundary mobility:

$$M_{\text{pure}} = \frac{\delta D_{GB} V_m}{b^2 R T} \quad [3]$$

In this equation, D_{GB} is the grain boundary self-diffusion coefficient, V_m is the molar volume, b is the magnitude of the Burgers vector, T is the absolute temperature, and R is the gas constant. The grain boundary diffusion coefficient was estimated from the bulk diffusion coefficient by using activation energy Q_{GB} , which is 2/3 that of bulk diffusion.^[12,19] The best fit of the experimental data was obtained using a mobility that is 1/3 the Turnbull estimate. This is not surprising given the fact that the Turnbull mobility does not take into account attachment kinetics and is, therefore, an overestimate of the actual mobility. Therefore, the mobility used in this work is

$$M_{\delta}(t) = \frac{0.7075}{T(t)} \times \exp\left(\frac{-20995.43}{T(t)}\right) \quad [4]$$

In order to evaluate the integral in Eq. [2], an expression for the temperature as a function of time is needed. This was obtained experimentally from the data recorded by the thermocouple attached to each specimen.

The results of this simple model are compared to the experimental data on delta grain growth at 1273 K (1000 °C), 1373 K (1100 °C), 1473 K (1200 °C), 1573 K (1300 °C), and 1743 K (1470 °C) in Figure 8. In general, excellent agreement is obtained between the experimental data and the model predictions. It is noted that the model overestimates the grain size at the longest times. This is believed to be due to the fact that at long times the grain size becomes comparable to the sample thickness (2.5 mm) and the measured grain-growth kinetics no longer represents grain growth in the bulk. The fact that the data could be fitted with the present model, which does not include Zener pinning or solute drag, adds further support to the argument that the addition of the Al does not significantly change the rate of grain growth in delta-ferrite; the role of Al is simply to stabilize delta-ferrite down to room temperature. The results obtained here are, therefore, applicable to delta grain growth in APIX60 steels.

B. Grain Growth in Austenite

Austenite grain growth at 1573 K (1300 °C) and 1673 K (1400 °C) could be modeled using the simple description of Section A, provided that the initial austenite grain size is known. The challenge here is that the alloy consists of a mixture of ferrite and pearlite at room temperature. Austenite will be formed on heating. In order to bypass this complication, the integral in Eq. [2] was evaluated from t_1 to t , where t_1 is the time at which the temperature has reached 1173 K (900 °C). Consequently, the initial radius, r_0 , should now be the

radius when the temperature is 1173 K (900 °C), which was taken to be $40 \mu\text{m}$, as shown in Figure 3. Finally, it was necessary to estimate the mobility of the austenite grain boundaries. Once again the grain-boundary diffusion coefficient was estimated from the bulk diffusion coefficient ($Q_{GB} = 0.61Q$).^[12,19] The best fit of the experimental data was obtained with a mobility that is 0.3 times the Turnbull estimate:

$$M_{\gamma}(t) = \frac{0.1920}{T(t)} \times \exp\left(\frac{-20837.14}{T(t)}\right) \quad [5]$$

The results are shown in Figure 9 and appear to be in good agreement with the experimental data.

C. Application to TSCDR

During typical TSCDR practice, large TiN particles are formed in the liquid during the late stages of solidification. After the caster, before leaving the homogenization furnace, the titanium-nitride precipitates will keep on coarsening because of the change of the solubility of TiN.^[20] These large precipitates exert a small Zener pinning effect. Strong Zener pinning conditions are not encountered until fine Nb(C,N) precipitates are formed during thermomechanical processing.^[21,22] For this reason, our results on the precipitate-free model alloys can be used to model the grain-size evolution during TSCDR up to the point where the slabs exit the homogenization furnace and the thermomechanical processing begins.

A key point that needs to be considered is that the cooling rate varies from the slab surface to the slab center, leading to variations in the microstructure evolution and grain size. The normal grain-growth model developed in this contribution can be used to calculate delta and austenite grain growth at different positions in the slab. Table II lists the relevant transformation temperatures for APIX60, as calculated from the TCFE2 database of THERMO-CALC.^[13] We have not attempted to model the delta to gamma transformation. Instead we simply assumed that the delta grain growth occurs down to 1743 K (1470 °C) and austenite grain growth occurs at lower temperatures. The initial delta-ferrite grain size is taken to be the secondary dendrite arm spacing (SDAS). This was experimentally measured near the surface and at the center of the thin slab provided by Nucor (Nucor Steel Decatur, LLC, Trinity, AL). Linear variation of the dendrite arm spacing with slab thickness was assumed, as shown in Figure 10(a). The initial austenite grain size was assumed to be smaller than the final delta grain size by a factor of 3,^[23] which allowed us to capture the effect of grain refinement due to the delta to gamma transformation. Finally, a validated heat-transfer model from Nucor was used to estimate the cooling rate at each point of the slab. For example, the cooling rates at the surface, 20 mm below the surface, and the center of the slab are shown in Figure 10(b).

Figure 11(a) shows the predicted delta grain size as a function of position, just before the onset of the delta to gamma transformation. The solid diamonds are the

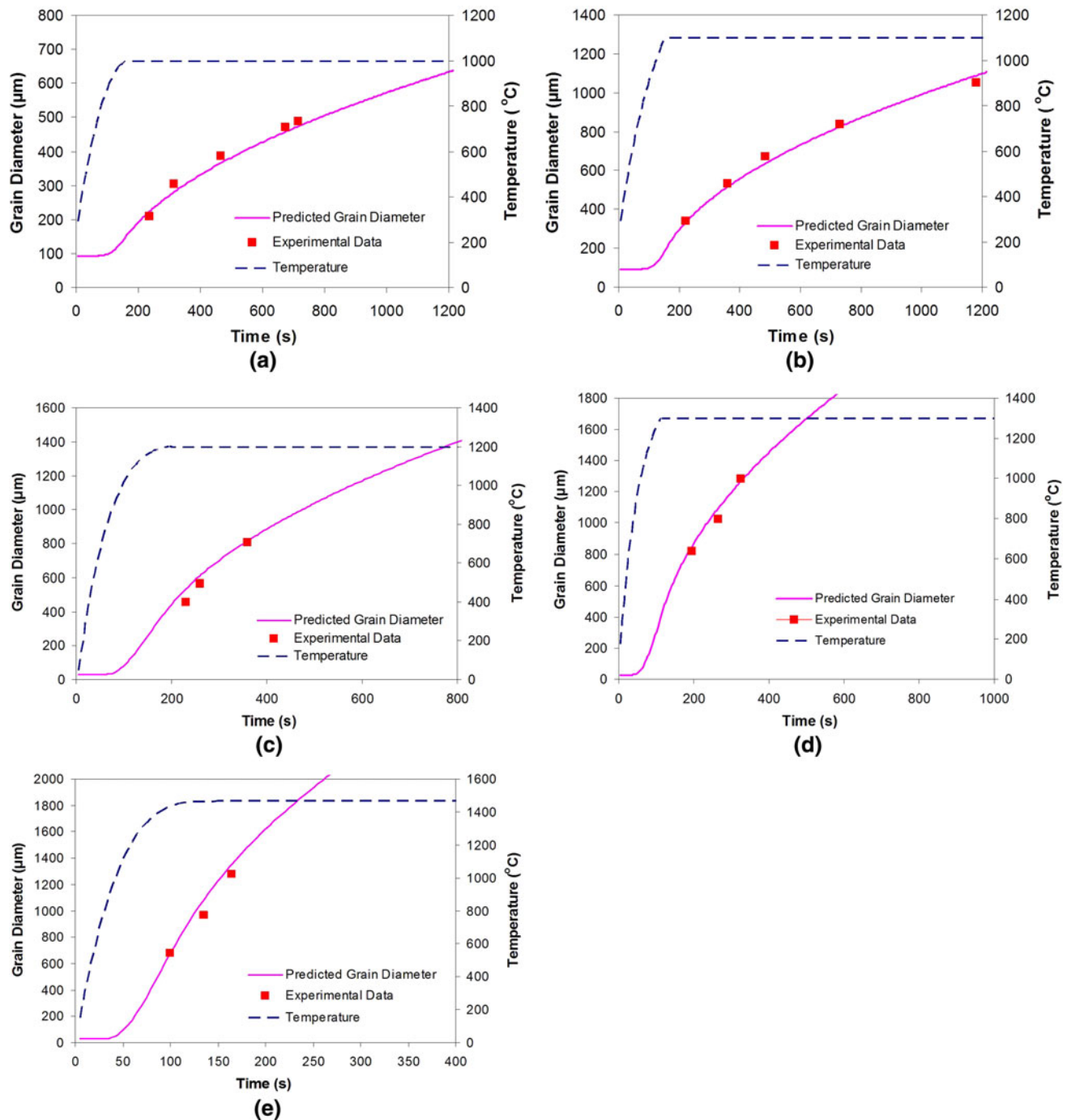


Fig. 8—Comparison of the measured and predicted delta grain-growth kinetics at (a) 1273 K (1000 °C), (b) 1373 K (1100 °C), (c) 1473 K (1200 °C), (d) 1573 K (1300 °C), and (e) 1743 K (1470 °C). The heating rate curve is shown on the secondary axis.

calculated delta grain sizes at the slab surface, as well as 5, 10, 20, and 30 mm below the surface, and at the slab center. The solid line is used to highlight the trends of grain size change with the distance from surface of the slab. In addition, one can calculate the austenite grain size that would be expected when the slab is about to enter the homogenization furnace (Figure 11(b)) and grain size upon leaving the homogenization furnace (Figure 11(c)). The solid symbols and solid lines have the same meaning as previously noted. The predicted gamma grain size as a function of slab thickness as the

slab leaves the homogenization furnace can be compared to industrial samples obtained from the slab after leaving the homogenization furnace; an example of such data is also shown in Figure 11(c) for comparison.^[6] Very good agreement is obtained between the predicted and measured austenite grain size as a function of position. This lends further support to the simple grain-growth treatment used here.

The results of Figure 11 show that the austenite grain size before entering the homogenization furnace is nonuniform with finer grains being present near the

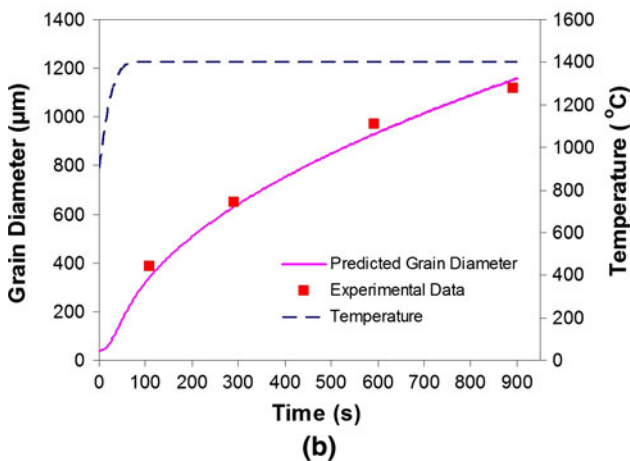
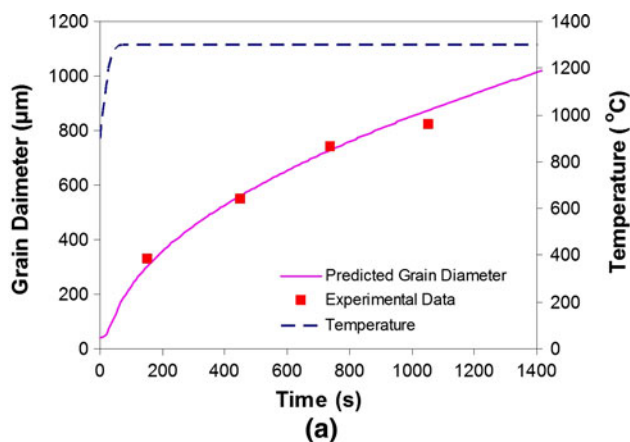


Fig. 9—Comparison of the measured and predicted austenite grain-growth kinetics of Nb/Ti-free alloy at (a) 1573 K (1300 °C) and (b) 1673 K (1400 °C); the time evolution of the specimen temperature is shown on the secondary axis.

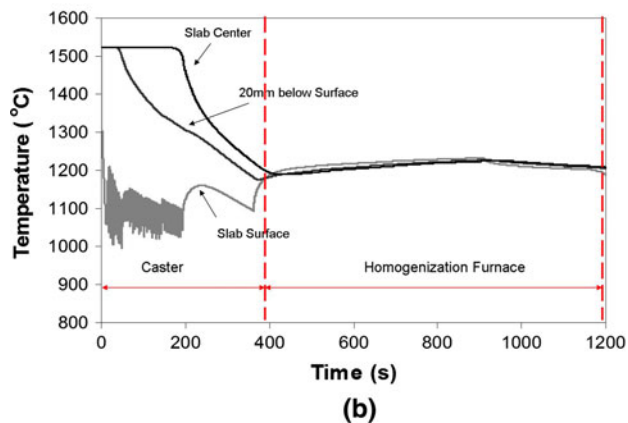
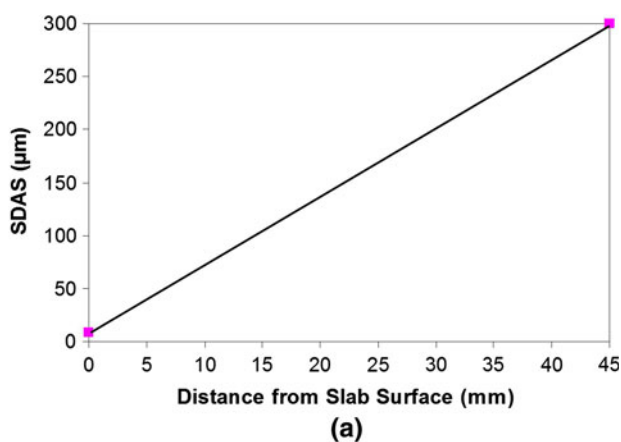


Fig. 10—(a) Secondary dendrite arm spacing as a function of position within the APIX60 slab. The solid line is based on the interpolation of two measurements made in this investigation. (b) Cooling curves at the surface, 20 mm below the surface and the center of the slab, as provided by Nucor.

Table II. Phase Transformation Temperature of APIX60

| | | | | | |
|----------------------|------------------|------------------------------------|------------------------------------|------------------------------------|--|
| Temperature (K (°C)) | >1797.5 (1524.5) | 1797.5 (1524.5) to 1769.8 (1496.8) | 1769.8 (1496.8) to 1750.5 (1477.5) | 1750.5 (1477.5) to 1721.0 (1448.0) | 1721.0 (1448.0) to 1721.0 (1448.0) to 1125.0 (852.0) |
| Phase | liquid | liquid + delta | delta | delta + gamma | gamma |

surface. After homogenization at 1473 K (1200 °C), which is above the precipitate pinning temperature for the present steel (APIX60), the grains at the surface grow significantly and become comparable in size to those at the center of the slab. If a lower homogenization temperature or higher microalloying content is used, it is possible to pin grain growth in the homogenization furnace. This, however, would lead to a nonuniform grain size distribution, with large grains in excess of 800 μm being present at the center. This seems to be the case in higher grade API steels (*e.g.*, X80), where it is often reported that the grain size at the center is significantly larger than that at the surface of the slab.

Another important consequence of the results shown in Figure 11 is that grain-size control in both the delta and austenite is necessary in order to avoid the presence of excessively large grains at the center of the slab in

the TSCDR process. Some variation in grain-size between the surface and the center of the slab will still be present, as this is inherited from the as-cast structure (Figure 10(a)).

It seems that future research efforts should focus on developing effective pinning methods for preventing grain growth in delta-ferrite and austenite prior to thermomechanical processing. This is a challenging task because rapid precipitate coarsening would be expected at high temperatures. Various oxide dispersions have been suggested for this purpose.^[24]

V. CONCLUSIONS

1. Delta-ferrite grain growth was studied using a model alloy in which delta-ferrite is stable down to room

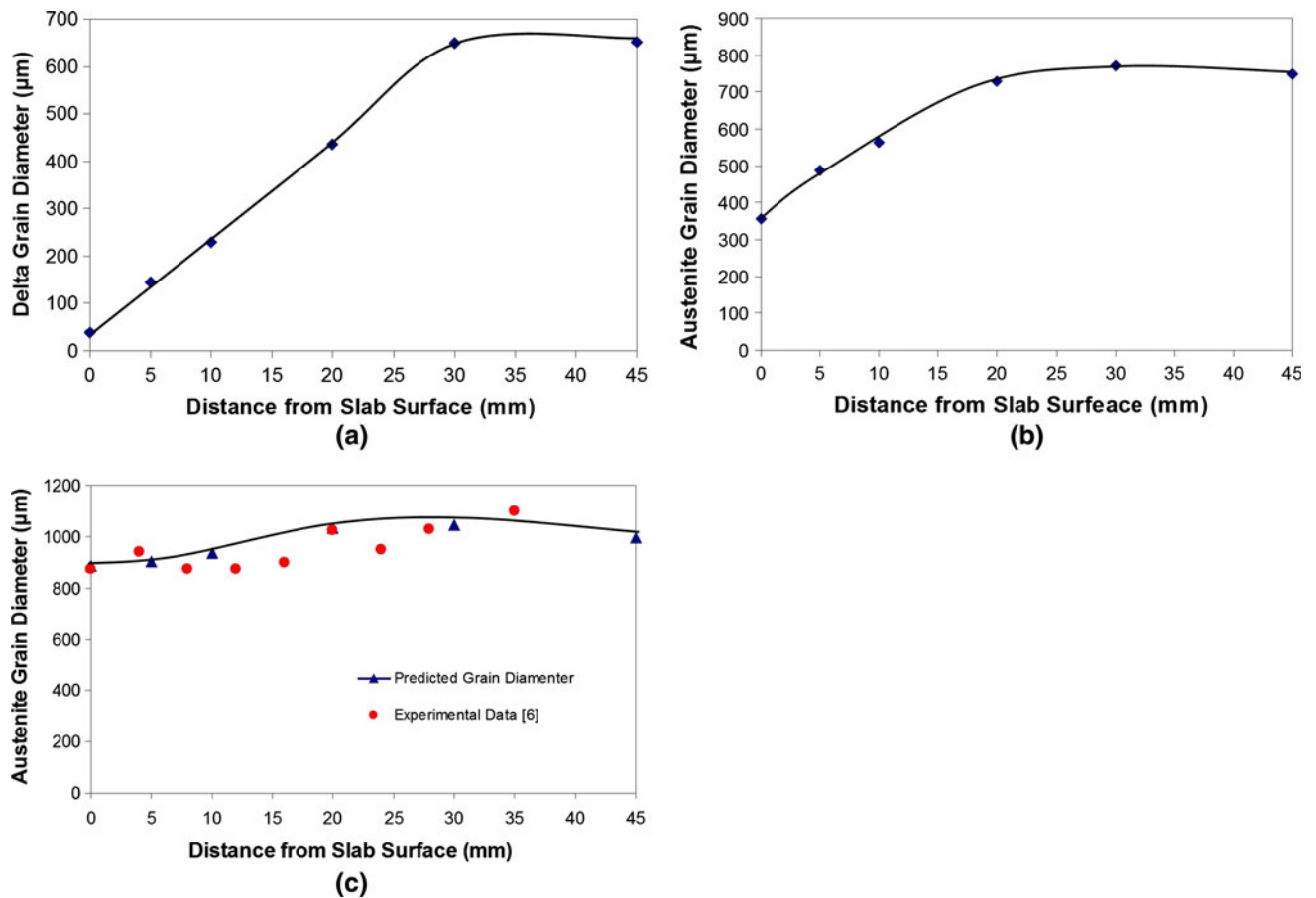


Fig. 11—(a) Predicted delta grain size as a function of slab position just before the onset of the delta to gamma transformation. (b) Predicted austenite grain size when the slab is about to enter the homogenization furnace. (c) Comparison of the predicted and experimentally measured^[6] gamma grain size as the slab leaves the homogenization furnace.

temperature. The results were modeled using a simple nonisothermal grain-growth model.

2. Austenite grain growth was investigated at temperatures between 1473 K (1200 °C) and 1673 K (1400 °C) using Nb/Ti-free alloy to bypass the complications of particle pinning and abnormal grain growth. Grain-growth kinetics at 1573 K (1300 °C) and 1673 K (1400 °C) was successfully described using a model similar to that used to model grain growth in delta-ferrite.
3. Application of the model to grain growth in APIX60 successfully reproduced the grain size distribution as a function of position within the slab. The results suggest that it is essential to control grain growth in both delta-ferrite and austenite in order to maintain a grain size of less than 400 μm prior to the onset of thermomechanical processing.

ACKNOWLEDGMENTS

Mr. J. Thomson, McMaster University, is gratefully acknowledged for valuable discussions. We are

also grateful for the support of the McMaster Steel Research Centre.

REFERENCES

1. M. Korchynsky: *33rd McMaster Symp. on Iron & Steelmaking: Thinner Slab Casting*, G.A. Irons, ed., McMaster University, Hamilton, 2005, pp. 251–59.
2. J. Muller, W. Henning, and C. Bilgen: *33rd McMaster Symp. on Iron & Steelmaking: Thinner Slab Casting*, G.A. Irons, ed., McMaster University, Hamilton, 2005, pp. 240–50.
3. R. Wang, C.I. Garcia, M. Hua, H. Zhang, and A.J. DeArdo: *Mater. Sci. Forum*, 2005, vols. 500–501, pp. 229–36.
4. P. Uranga, A.I. Fernández, B. López, and J.M. Rodriguez-Ibabe: *Mater. Sci. Forum*, 2005, vols. 500–501, pp. 245–52.
5. C.P. Reip, W. Hennig, J. Kempken, and R. Hagmann: *Mater. Sci. Forum*, 2005, vols. 500–501, pp. 287–94.
6. H. Zhang, G. Pan, R. Wang, and C. Liu: *Mater. Sci. Forum*, 2005, vols. 500–501, pp. 295–300.
7. A. Bakkaloglu: *Mater. Lett.*, 2002, vol. 56, pp. 200–09.
8. G. Zhu and S.V. Subramanian: *Mater. Sci. Eng. A*, 2006, vol. 426, pp. 235–39.
9. P.D. Hodgson, H. Beladi, and M.R. Barnett: *Mater. Sci. Forum*, 2005, vols. 500–501, pp. 39–48.
10. M. Gómez and S.F. Medina: *Mater. Sci. Forum*, 2005, vols. 500–501, pp. 147–54.
11. N.S. Pottore, C.I. Garcia, and A.J. DeArdo: *Metall. Mater. Trans. A*, 1991, vol. 22A, pp. 1871–80.

12. T. Gladman: *The Physical Metallurgy of Microalloyed Steel*, Institute of Materials, London, 1997, pp. 159–61.
13. Available from THERMO-CALC software, www.thermocalc.com.
14. C. Zener: quoted by C. Smith, *Trans. AIME*, 1948, vol. 175, pp. 15–51.
15. J.W. Cahn: *Acta Metall.*, 1962, vol. 10, pp. 789–98.
16. H.S. Zurob, C.R. Hutchinson, Y. Brechet, and G. Purdy: *Acta Mater.*, 2002, vol. 50, pp. 3075–92.
17. F.J. Humphreys and M. Hatherly: *Recrystallization and Related Annealing Phenomena*, 2nd ed., Elsevier Ltd., Oxford, UK, 2004, pp. 335–36.
18. D. Turnbull: *Trans. AIME*, 1951, vol. 191, pp. 661–65.
19. D.S. Wilkinson: *Mass Transport in Solids and Fluids*, Cambridge University Press, Cambridge, UK, 2000, pp. 37–39.
20. M.T. Nagata, J.G. Speer, and D.K. Matlock: *Metall. Mater. Trans. A*, 2002, vol. 33A, pp. 3099–3110.
21. O. Kwon and A.J. DeArdo: *Acta Metall.*, 1991, vol. 39, pp. 529–38.
22. E.J. Palmiere, C.I. Garcia, and A.J. DeArdo: *Metall. Mater. Trans. A*, 1994, vol. 25A, pp. 277–86.
23. H. Yin, T. Emi, and H. Shibata: *Acta Mater.*, 1999, vol. 47, pp. 1523–35.
24. H. Suito, H. Ohta, and S. Morioka: *ISIJ Int.*, 2006, vol. 46, pp. 840–46.